Nickel Colloids in Reduced Nickel-Doped Magnesium Oxide

J. Narayan, Y. Chen, and R. M. Moon
Solid State Division, Oak Ridge National Laboratory, Oak Ridge, Tennessee 37830

(Received 14 November 1980)

High-temperature treatment in a reducing atmosphere of Ni-doped MgO crystals resulted in the formation of colloids with an average size of about 50 nm. The colloids are coherent nickel precipitates having a fcc structure ($a = 0.352$ nm), and occasionally a bcc structure ($a = 0.288$ nm). The ratio of magnetic to nuclear scattering amplitudes for the (111) precipitate reflection was about 17% below the value for nickel. Optical absorption measurements indicate that a broad optical band centered at ~2.2 eV is associated with the colloidal precipitates.

PACS numbers: 81.10.Fq, 61.12.Dw, 61.16.Di, 61.70.Dx

Colloidal precipitates with diameters in the range 1–200 nm in ionic crystals lead to interesting modifications of physical properties of these materials.[1] Mechanical properties (yield stress and ductility), selective absorption of solar energy, cathodochromic, photochromic, and data-storage applications represent a few examples of effects produced by colloids.[1] Since these colloids are formed by a nucleation and growth process inside a given lattice, their shape, structure, and properties could strongly be influenced by the crystal structure of the host lattice. Most of the previous studies on metal colloids were concentrated on halides.[1,2] Potassium, sodium, and lithium colloids have been reported in the near-surface regions of MgO after ion implantation and subsequent heat treatment.[3,4] Detailed information on colloidal precipitates has been lacking because of the inadequacy of conventional techniques of electron microscopy, which were used in the previous experiments. In the present investigation, analytical electron microscopy and neutron-magnetic scattering techniques were used, providing detailed information on the structure, morphology, and chemical composition of small precipitates.[5,6] This Letter has a twofold purpose. First, we provide direct evidence of the presence of colloids in reduced (additive coloration[7,8]) nickel-doped MgO. Second, we show that these are metallic nickel precipitates with a normal fcc structure, but under fast-quenching conditions a fraction of them have a new bcc structure.

Nickel-doped (100) magnesium oxide crystals were prepared by an arc-fusion technique[9] with use of MgO powder (obtained from Kanto Chemical Company) mixed with NiO powder to about 5% in weight. Spectrographic analysis showed that the resulting crystals contained about 0.4 at.% nickel impurity. As-grown crystals exhibited a slightly greenish color associated with Ni^{2+} ions in substitutional sites. Clustering of nickel into precipitates (formation of colloids) was achieved by heating the Ni-doped crystal at ~2100 K in a strongly reducing atmosphere and subsequently cooling these crystals rapidly. The reducing atmosphere used in the present work was magnesium vapor (pressure ~6 atm) in a tantalum capsule (bomb). Recently, some clustering of nickel has also been obtained in CO_2 or N_2 atmosphere in a graphite capsule.[10]

The diffraction analysis of individual precipitates was carried out with use of the STEM (scanning transmission electron microscope) attachment in a Philips EM-400 analytical electron microscope, the electron optics of which results in electron probe diameters <5 nm. Thus, it is possible to obtain diffraction information from areas of the order of 10 nm in diameter, which is significantly smaller than the ~300 nm diameter obtainable in the selected area diffraction technique used in conventional low-voltage electron microscopy. The specimens were also analyzed with use of x-ray dispersive analysis to determine the chemical composition of individual precipitates. Magnetic scattering experiments were performed with a polarized–neutron-beam spectrometer installed at the Oak Ridge National Laboratory high-flux isotope reactor. The optical absorption spectra were measured with Cary-17*D* spectrophotometer.

As-grown crystals of Ni-doped MgO contained no precipitates down to the microscope resolution limit of about 1 nm, with the exception of a very small number of precipitates at subgrain-boundary dislocations. The precipitation at the subboundaries is a normal occurrence[10,11] in melt-grown ionic crystals due to the electric potentials associated with the dislocations. After reducing the as-grown crystals in the tantalum bomb, a high concentration of precipitates or colloids is

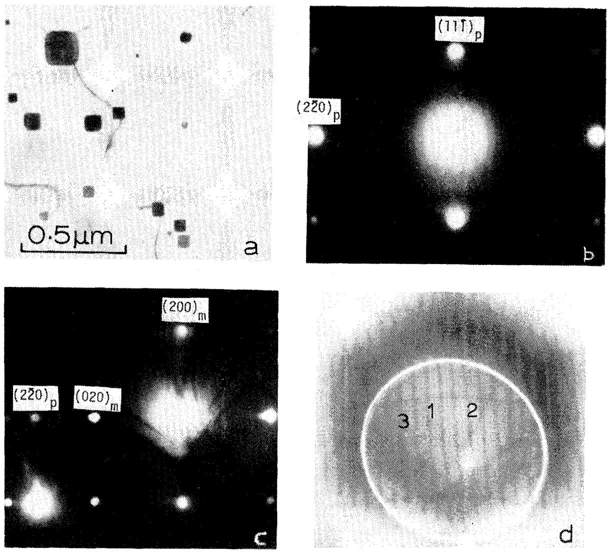

FIG. 1. Electron micrographs for the analysis of colloids. (a) Bright-field electron micrograph showing the size distribution and moiré fringes associated with the precipitates. (b) (112) fcc microdiffraction pattern from a precipitate near the edge. (c) (112) precipitate and (100) matrix diffraction patterns superimposed. (d) (111) fcc nickel convergent-beam diffraction pattern where 1, 2, and 3 represent $(\bar{5}\bar{3}9)$, $(\bar{3}\bar{5}9)$, and $(\bar{7}71)$ HOLZ lines, respectively.

TABLE I. d_{hkl} values from diffraction patterns in different orientations.

Colloidal precipitate		MgO matrix	
hkl	d_{hkl} (nm)	*hkl*	d_{hkl} (nm)
111	0.204 ± 0.001	111	0.242 ± 0.001
200	0.176	200	0.210
220	0.124	220	0.148
311	0.106	311	0.126
222	0.102	222	0.121
400	0.083	400	0.105
		331	0.096

observed as shown in Fig. 1(a), which is a bright-field micrograph obtained with use of the [200] diffraction vector ($\bar{g}$). The average size (first moment) of the precipitates was determined (foil thickness ~0.5 µm) to be 50 nm with number density 1.0×10^{19} m^{-3}. With use of both stereomicroscopy and tilting experiments, the precipitates were analyzed to be cubes with truncated corners.

Fig. 1(b) shows a microdiffraction pattern from a precipitate with the electron-beam direction being close to the MgO matrix normal [001]. This precipitate was located near the edge of the specimen so that we could obtain diffraction information from the precipitate only. The diffraction pattern shown in Fig. 1(c) was obtained from a precipitate which was inside the matrix. In this case precipitate diffraction spots (p) are similar to those in Fig. 1(b) and matrix spots (m) correspond to the (001) orientation. When this specimen was tilted 19.5° around the [010] axis of the matrix, a spot diffraction pattern from the precipitate near the edge of the specimen exhibited a threefold or a sixfold symmetry. However, a convergent-beam diffraction (CBD) pattern from this precipitate contained only threefold symmetry. The CBD patterns provide information on the three-dimensional symmetry of materials and are very useful for unequivocal determination of symmetry and space groups. The indexed CBD pattern showing $(\bar{5}\bar{3}9)$, $(\bar{3}\bar{5}9)$, and $(\bar{7}71)$ higher-order Laue zones (HOLZ) lines in Fig. 1(d) is similar to the (111) pattern for fcc nickel.[11,12] Lattice spacings of planes (d_{hkl}) corresponding to various diffraction spots were determined by the relation $rd_{hkl}=C$, where r is the distance in the diffraction pattern between the central and the diffracting beams, and C is the diffraction contrast measured with use of matrix spots or by a standard Au specimen. Precipitate d_{hkl} values obtained from diffraction patterns in different orientations are given in Table I. These d_{hkl} correspond to a simple fcc structure with a lattice constant (a_0) of 0.352 nm, the same as that of bulk nickel. From the symmetry and the d_{hkl} corresponding to various precipitate diffraction spots in Figs. 1(b) and 1(c), we could uniquely index them to be the (112) pattern of fcc nickel. From these patterns we deduced the following precipitate (p) and matrix (m) orientation relationships for a given precipitate: $[11\bar{1}]_p \parallel [100]_m$, and $[1\bar{1}0]_p \parallel [010]_m$.

The precipitates exhibited black-white contrast under dynamical diffraction conditions indicating the presence of unrelaxed coherency strains. Moiré patterns resulting from the interference between {111} precipitate and {200} matrix planes are shown in Fig. 1(a), which was obtained with use of the [200] matrix diffraction vector ($\bar{g}$). With $\bar{g}=[020]$, precipitates with $[11\bar{1}]_p \parallel [020]_m$ showed similar moiré fringes. These moiré or interference patterns represent periodicity with which the planes at the interface of the precipitate and the matrix go in and out of register.[5] From a moiré spacing of 7.0 nm, and with use of a value of 0.210 nm for the matrix

d_{200}, the d_{111} for the precipitate is calculated to be 0.204 nm, which is in good agreement with the value obtained from the diffraction patterns.

X-ray fluorescence studies performed on individual precipitates indicated mostly the presence of nickel. The fluorescence studies were performed on precipitates near the edge of the specimen where there was no MgO present. Integrated intensity counts on these precipitates, after subtracting similar counts from a hole, to obtain the background (the microscope specimen contained a hole with a surrounding area transparent to electrons), gave a ratio for nickel of 99, indicating that the precipitates are composed of (99 ± 1)% nickel.[11]

The neutron scattering experiment consisted of measuring the intensity in a $(111)_p$ peak when the incident neutrons were polarized parallel and then antiparallel to the sample magnetization. The precipitates were magnetically saturated by applying an external magnetic field of 12 kOe. The ratio of these intensities, which is called the flipping ratio, is given by

$$R=[(1+p/b)/(1-p/b)]^2, \qquad (1)$$

where p and b are, respectively, the magnetic and nuclear scattering amplitudes. The flipping ratio for the (111) precipitate reflection at room temperature resulted in a p/b value of 0.099 ± 0.002, which should be compared with 0.119 for pure-nickel metal.[13] This difference implies that the average nickel moment in the precipitates is smaller than that in pure-nickel metal by 17%. This may be attributed to one or more of the following possible causes: (1) impurities in the precipitates, (2) a magnetically "dead" layer at the surface of the precipitates, or (3) the presence of other nickel phases (see below) with different magnetic properties than the fcc phase. The d_{hkl} values determined from the neutron diffraction pattern for (111), (200), and (220) precipitate reflections were in excellent agreement with the values in Table I. These experiments also gave the precipitate-matrix orientation relationship, which was the same as that determined by electron microscopy.

The optical absorption spectra (absorption coefficient, α, versus wavelength, λ) at 77 K for specimens similar to those used for electron and neutron scattering measurements are shown in Fig. 2. The main features of the spectrum of as-grown crystals [shown in Fig. 2(a)] are due to the substitutional Ni^{2+} ions.[14] After the reduction, these crystals turned dark and almost opaque. A broad and intense band centered near 2.0 eV is observed and is attributed to nickel colloids.[15] The metallic colloids modify the absorption spectra of oxides in such a way that these materials are ideally suited for efficient solar-energy absorption. An ideal solar absorber is characterized by high α for $\lambda \lesssim 2.0$ μm, and low α and emissivity for $\lambda \gtrsim 2.0$ μm to retain the absorbed energy. The optical spectra of these materials were found to be unchanged after a long (100 h) time of annealing at 1073 K, thus making them suitable for high-temperature, solar-absorber applications. Such materials are not presently available.

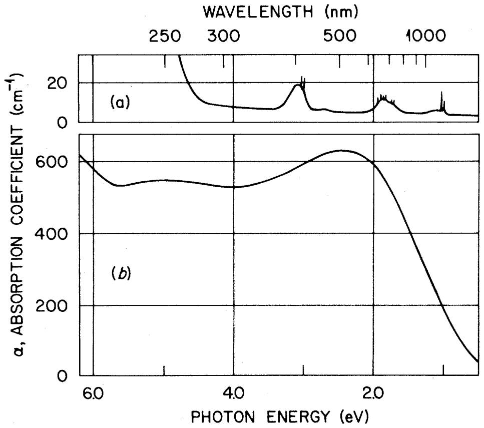

FIG. 2. Optical spectra of Ni-doped MgO crystals: (a) from as-grown Ni-doped MgO crystals at 77 K; (b) after reduction in a Ta bomb at 2000 K in the presence of Mg vapor.

The precipitates frequently contained small regions (10–20 nm wide) with a high density of stacking faults. The structure of these regions was determined (with use of "micro"-microdiffraction techniques) to be hexagonal-close-packed (hcp). The hcp structure of nickel has been reported in the case of certain thin film deposits.[16] Under fast quenching conditions we also found that a fraction of the nickel precipitates had a body-centered-cubic structure. The d_{110} for the bcc nickel was determined with use of diffraction and moiré-pattern analyses and it was found to be 0.204 nm corresponding to $a_0 = 0.288$ nm. It was interesting to note that the d_{110} for the bcc structure was equal to the d_{111} for the fcc structure of nickel. These precipitates had a following orientation relationship with the matrix: $[\bar{1}10]_p \parallel [100]_m$, and $[\bar{1}\bar{1}2]_p \parallel [010]_m$.

In conclusion, we have established the presence of nickel colloidal precipitates in nickel-doped MgO after a high-temperature reduction. The structure of these precipitates was determined to be fcc with $a_0 = 0.352$ nm, and $[11\bar{1}]_p \parallel [100]_m$, and $[1\bar{1}0] \parallel [010]$ relationship with the matrix. The new bcc phase of nickel had $a_0 = 0.288$ nm with $[\bar{1}10]_p \parallel [100]_m$, and $[\bar{1}\bar{1}2] \parallel [010]$ relationship with the matrix. The ratio of magnetic to nuclear scattering amplitudes (0.099 ± 0.002) for the (111) reflection of the precipitates is 17% below the value reported for pure-nickel metal. The optical absorption spectrum from this material is characteristic of the presence of metallic precipitates. The optical spectrum containing an absorption edge at $\lambda \approx 2.0$ μm makes these materials ideally suited for efficient solar absorption.

This research was sponsored by the Division of Materials Sciences, U. S. Department of Energy under Contract No. W-7405-ENG-26 with Union Carbide Corporation.

---

[1] A. E. Hughes and S. C. Jain, Adv. Phys. 28, 717 (1979).

[2] S. Amelinckx, in *The Direct Observations of Dislocations*, Supplement No. 6 to Solid State Physics, edited by F. Seitz and D. Turnbull (Academic, New York, 1964).

[3] M. Treilleux, P. Thevenard, G. Chassange, and L. W. Hobbs, Phys. Status Solidi (a) 48, 425 (1978).

[4] M. Treilleux and G. Chassange, J. Phys. Lett. (Paris) 40, L161 (1979).

[5] J. Narayan, M. M. Abraham, Y. Chen, and H. T. Tohver, Philos. Mag. 38, 247 (1978).

[6] H. R. Kerchner, J. Narayan, D. K. Christen, and S. T. Sekula, Phys. Rev. Lett. 44, 1146 (1980).

[7] Y. Chen, J. L. Kolopus, and W. A. Sibley, Phys. Rev. 186, 865 (1969).

[8] K. L. Lee and J. H. Crawford, Phys. Rev. B 15, 4065 (1977).

[9] M. M. Abraham, C. T. Butler, and Y. Chen, J. Chem. Phys. 55, 3752 (1971).

[10] J. Narayan, unpublished.

[11] J. Narayan and Y. Chen, J. Appl. Phys. 51, 1242 (1980).

[12] J. W. Steeds, in *Introduction to Analytical Electron Microscopy*, edited by J. J. Hren, J. I. Goldstein, and D. C. Joy (Plenum, New York, 1979), Chap. 15.

[13] H. A. Mook, Phys. Rev. 148, 495 (1966).

[14] M. V. Iverson, J. C. Windscheif, and W. A. Sibley, Appl. Phys. Lett. 36, 183 (1980).

[15] Y. Chen, unpublished.

[16] L. A. Bruce and H. Jaeger, Philos. Mag. 36, 1331 (1977).

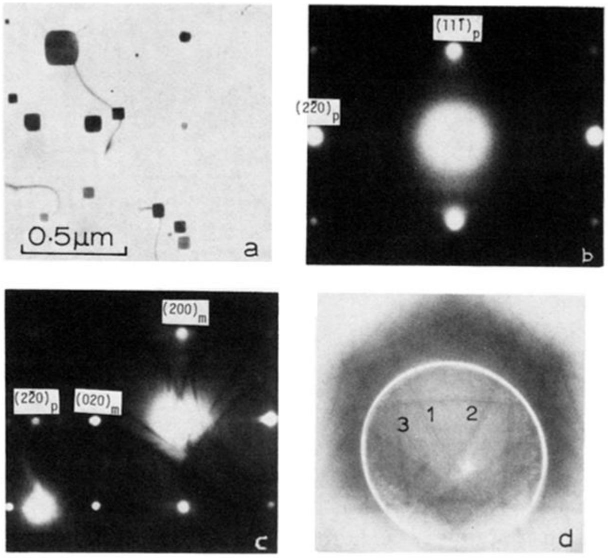

FIG. 1. Electron micrographs for the analysis of colloids. (a) Bright-field electron micrograph showing the size distribution and moiré fringes associated with the precipitates. (b) (112) fcc microdiffraction pattern from a precipitate near the edge. (c) (112) precipitate and (100) matrix diffraction patterns superimposed. (d) (111) fcc nickel convergent-beam diffraction pattern where 1, 2, and 3 represent $(\bar{5}\bar{3}9)$, $(\bar{3}\bar{5}9)$, and $(\bar{7}71)$ HOLZ lines, respectively.